PLOS ONE

RESEARCH ARTICLE

T vector velocity: A new ECG biomarker for identifying drug effects on cardiac ventricular repolarization

Werner Bystricky[1]*, Christoph Maier[1,2], Gary Gintant[3], Dennis Bergau[1], Kent Kamradt[1], Patrick Welsh[1], David Carter[1]*

1 Clinical Pharmacology, AbbVie Inc., North Chicago, Illinois, United States of America, **2** Department of Medical Informatics, Heilbronn University, Heilbronn, Germany, **3** Integrated Sciences and Technology, AbbVie Inc., North Chicago, Illinois, United States of America

* werner.bystricky@abbvie.com (WB); david.carter@abbvie.com (DC)

Citation: Bystricky W, Maier C, Gintant G, Bergau D, Kamradt K, Welsh P, et al. (2019) T vector velocity: A new ECG biomarker for identifying drug effects on cardiac ventricular repolarization. PLoS ONE 14(7): e0204712. https://doi.org/10.1371/journal.pone.0204712

Editor: Randall Lee Rasmusson, University at Buffalo - The State University of New York, UNITED STATES

Received: September 3, 2018

Accepted: June 4, 2019

Published: July 8, 2019

Data Availability Statement: The data used in this study is publicly available from http://physionet.org/physiobank/database/ecgrdvq/ and http://physionet.org/physiobank/database/ecgdmmld/.

Funding: This study was funded by AbbVie Inc. The funder provided support in the form of salaries for authors GG DB KK PW DC, and in the form of consultant fees for authors WB CM. The funder did not have any additional role in the study design, data collection and analysis, decision to publish, or

Abstract

Background

We present a new family of ECG biomarkers for assessing drug effects on ventricular repolarization. We show that drugs blocking inward (depolarizing) ion currents cause a relative increase of the T vector velocity (TVV) and accelerate repolarization, while drugs blocking outward ion currents cause a relative decrease of the TVV and delay repolarization. The results suggest a link between the TVV and the instantaneous change of the cellular action potentials that may contribute to bridge the gap between the surface ECG and myocardial cellular processes.

Methods

We measure TVV as the time required to reach **X**% of the total **Tr**ajectory length of the T vector loop, denoted as Tr*X*. Applied to data from two FDA funded studies (22+22 subjects, 5232+4208 ECGs) which target ECG effects of various ion-channel blocking drugs, the Tr*X* effect profiles indicate increasingly delayed electrical activity over the entire repolarization process for drugs solely reducing outward potassium current (dofetilide, moxifloxacin). For drugs eliciting block of the inward sodium or calcium currents (mexiletine, lidocaine), the Tr*X* effect profiles were consistent with accelerated electrical activity in the initial repolarization phase. For multichannel blocking drugs (ranolazine) or drug combinations blocking multiple ion currents (dofetilide + mexiletine, dofetilide + lidocaine), the overall Tr*X* effect profiles indicate a superposition of the individual Tr*X* effect profiles.

Results

The parameter Tr40c differentiates pure potassium channel blocking drugs from multichannel blocking drugs with an area under the ROC curve (AUC) of 0.90, CI = [0.88 to 0.92]. This is significantly better than the performance of J-T_{peak}c (0.81, CI = [0.78 to 0.84]) identified as the best parameter in the second FDA study. Combining the ten parameters Tr10c to Tr100c in a logistic regression model further improved the AUC to 0.94, CI = [0.92 to 0.96].

preparation of the manuscript. The specific roles of these authors are articulated in the 'author contributions' section.

Competing interests: W declare the following competing interests statements: Authors WB CM are consultants for AbbVie, Inc. and authors GG DB KK PW DC are employees of AbbVie Inc. This does not alter our adherence to PLOS ONE policies on sharing data and materials.

Conclusions

TVV analysis substantially improves assessment of drug effects on cardiac repolarization, providing a plausible and improved mechanistic link between drug effects on ionic currents and overall ventricular repolarization reflected in the body surface ECG. TVV contributes to an enhanced appraisal of the proarrhythmic risk of drugs beyond QTc prolongation and J-T_{peak}c.

Introduction

Drug effects on ion currents affecting the cardiac ventricular repolarization are well understood on the cellular level. On the ECG level, QTc prolongation is an established surrogate marker for Torsade-de-Pointes (TdP), and was introduced as an electrocardiographic biomarker standard for pro-arrhythmic risk assessment via regulatory pathways in 2005 [1]. Since that time, no drugs have been withdrawn from the market due to unexpected induction of TdP, demonstrating that QTc shows good sensitivity in identifying potentially dangerous compounds. However, a major point of criticism relates to the well-known lack of specificity of QTc, which may result in early discontinuation of promising candidate drugs.

Since pro-arrhythmic drugs can affect ECG morphology, a number of repolarization biomarkers have been proposed for the detection of waveform morphology abnormalities [2, 3] including T-wave duration measures [4], area or amplitude-based measures [5], measures based on a vectorcardiographic representation of the ECG [6, 7, 8], or measures that capture symmetry, flatness or notching of the T wave [9, 10]. However, the predictive value of changes in ECG morphology has not been established [1], and little is known about how such morphological parameters are linked to the electrophysiological process at the cellular level [11].

Recently, members of the Comprehensive *in vitro* Proarrhythmia Assay (CiPA) initiative [12] have completed two FDA-sponsored studies which addressed (1) the effect of ion channel blocks on various ECG biomarkers [13, 14] and (2) differentiation of QTc prolonging drugs with TdP risk (elicited by blocking the outward potassium current) from QTc prolonging drugs with minimal proarrhythmic risk (characterized by a balanced block of inward and outward ion currents) [15, 16]. These studies will be referred to hereafter as (1) Study A and (2) Study B respectively.

The fourth component of the CiPA initiative aims to rule out unexpected ion channel drug effects that may have been missed in in-vitro pre-clinical assessments. According to [17] successful candidate CiPA biomarkers are required to provide information which extends beyond what is captured by the existing parameters PQ interval, QRS duration and QTc. Moreover, they must contribute to improved differentiation of selective hERG blocking drugs from multi-ion channel blocking drugs since block of additional ionic currents may compensate for the reduced outward current resulting from hERG/iKr current block to subsequently reduce the extent of QTc prolongation and risk of arrhythmia.

Studies A and B demonstrate that a block of the hERG/iKr current prolongs both the early phase of repolarization, as quantified by the J-T_{peak} interval, and the late repolarization phase (T_{peak}-T_{end} interval). In contrast, late sodium or calcium inward current blocks preferentially affects the early phase of repolarization, as quantified by shortening only the J-T_{peak} interval. Moreover, one of the study evaluations [14] shows that changes in T-wave morphology are directly related to the amount of hERG/iKr block, but are also seen in compounds affecting additional ion channels. The authors conclude that the J-T_{peak} interval represents the best

biomarker currently available with respect to differentiating pure hERG/iKr current block from multi-ion channel blocks [16]. Still, the reported sensitivity of 0.82 and specificity of 0.77 leave room for improvement, and a physiologic interpretation of the J-T_{peak} interval changes are not obvious. Conceptually, this interval is measured from the vector magnitude lead. Its assessment may be sensitive to noise and physiologic fluctuations in particular for flat or notched T-wave morphologies [18].

This paper introduces a new family of biomarkers based on the T vector velocity (TVV), the velocity at which the heart's dipole vector evolves along its spatial trajectory during ventricular repolarization. We define the parameters Tr*X* as the time that it takes to reach certain percentages *X* of the total T-loop trajectory length, and combine the drug-induced changes on the heart rate corrected parameters Tr10, Tr20,.., Tr100 in so-called Tr*X*c effect profiles. We describe the proposed method and the results of its application to the data of Studies A and B. A performance comparison with the existing biomarkers J-T_{peak} and QTc is given. The results substantiate a significant improvement for identifying drug effects on cardiac ventricular repolarization. They also indicate a promising role for this approach in assessing a drug's pro-arrhythmic potential, and in differentiating multi-channel blocks from pure hERG/iKr current blockades. Moreover, they suggest that drug-related alterations of the action potential (AP) can be linked to the Tr*X*c effect profile. We are confident that these new biomarkers represent a substantial contribution towards the accomplishment of the CiPA objectives, and will advance the establishment of a relationship between myocardial cellular processes and the ECG.

Material and methods

Study data

We use de-identified data from two FDA-sponsored studies that are publicly available from the PhysioNet website [19]. The first study (Study A) [13, 20] contains 5,232 ECGs of 22 healthy subjects (11♀, age: 26.9 ± 5.5 y, BMI 23.1 ± 2.6 kg/m^2) partaking in a randomized, double-blind, 5-period crossover clinical trial. Its aim was to investigate whether multichannel blocking drugs with different potentials for blocking potassium, late sodium, and calcium currents can be differentiated by their effect on the ECG. In the morning of each 24h treatment period, all subjects received a single dose of one of the drugs dofetilide (500 μg), quinidine sulfate (400 mg), ranolazine (1,500 mg), verapamil hydrochloride (120 mg), or placebo. ECGs were extracted at 16 pre-defined time-points (pre-dose and 0.5, 1, 1.5, 2, 2.5, 3, 3.5, 4, 5, 6, 7, 8, 12, 14, 24 h post-dose. The subjects rested in a supine position for 10 min during ECG extraction, and serum PK samples were taken at the end of the resting phase. The washout period between treatments was 7 days. For further details see [13].

The second study (Study B) [15, 21] contains 4,211 ECGs from a randomized, double-blinded, 5-period crossover clinical trial in 22 healthy subjects who differ from those in Study A (9♀, age: 26.1 ± 4.9 y, 69.9 ± 9.0 kg). It addresses the electrophysiological responses to hERG/iKR current blocking drugs with and without the addition of blockade of either late sodium or calcium current blocking drugs. The 5 treatment periods include dofetilide alone, mexiletine without and with dofetilide, lidocaine without and with dofetilide, moxifloxacin without and with diltiazem, and placebo. In each period, subjects were dosed 3 times per day in the morning (hour 0), afternoon (hour 4) and evening (hour 9.5) as described in Table 1. For details see [15].

Studies A and B, registered at ClinicalTrals.gov as NCT02308748 and NCT01873950, were performed at a phase I clinical research unit (Spaulding Clinical, West Bend, WI). Both studies were approved by the US Food and Drug Administration Research Involving Human Subjects

Table 1. Dosing schema for Study B (modified from [15]).

Treatment period	Morning dose	Afternoon dose	Evening dose
Placebo (Pla)	Pla	Pla	Pla
Dofetilide (Dof)	Pla	Dof	Dof
Mexiletine (Mex) + Dofetilide	Mex	Mex + Dof	Mex + Dof
Lidocaine (Lid) + Dofetilide	Lid	Lid + Dof	Lid + Dof
Moxifloxacin (Mox) + Diltiazem (Dil)	Mox	Mox	Mox + Dil

https://doi.org/10.1371/journal.pone.0204712.t001

Committee (RIHSC 13-011D and 14-022D) and the local institutional review board (Chesapeake IRB). All subjects gave written informed consent [13, 15].

In both studies, continuous 12 lead ECGs (Surveyor, Mortara Instrument, Milwaukee, WI) were recorded at a sampling rate of 500 Hz and an amplitude resolution of 2.5 uV. Triplicate 10-second ECGs were extracted at each time point using the Antares Software (AMPS LLC). The study data contain J-T_{peak} measurements, corrected for heart rate according to [13]. We used these values for comparison with our TVV-based parameters.

ECG processing

All ECG files were analyzed with eECG/ABBIOS (AbbVie, Inc.'s proprietary, validated, ECG analysis system) in a semi-automated manner. ECGs were reviewed to identify artifacts, abnormal heartbeats, and unreliable automated annotations. ECGs of concern were manually reviewed to identify and annotate a minimum of 3 heartbeats per ECG with unaffected T-waves and consistent T annotations. The average RR intervals and the Fridericia corrected QT (QTcF) intervals [22] were extracted and used for further analyses.

For each ECG, the 12 lead signals were adjusted to the isoelectric lines (defined by the median amplitude of the PQ interval and interpolated between the heart beats by a cubic spline, see [23]), low-pass filtered (bidirectional Bessel filter with 36 Hz), and exported as an annotated ECG file in HL7 format (aECG) with 500 Hz sampling frequency, including the P, Q, J, and T_{end} annotations. The aECG files were loaded into, and further processed using the R system [24]. The supporting information S3 Text compares the resulting QTcF interval data from our analyses with the published QTcF data [13].

20 ECGs of Study A contained isolated leads that were strongly corrupted by noise. Those individual leads were set to zero. Since our approach aims at characterizing spatiotemporal properties of the cardiac repolarization process, we reconstructed the vectorcardiogram (VCG) by means of the inverse Dower transformation [25], and extracted the T-loop by limiting the VCG to the repolarization time interval [J + 20ms; T_{end}]. The rationale for choosing the Dower matrix is described in the supporting information S1 Text. Only normal sinus beats were used in subsequent analyses.

Calculation of TVV and T vector trajectory quantiles Tr*X*

Fig 1 illustrates the derivation of the TVV as the temporal derivative of the spatial T vector trajectory. The sequence of blue arrows represents a stroboscopic view in steps of 20 ms of the heart vector's temporal evolution during repolarization. In continuous time, the tip of the blue vectors inscribes the black trajectory, which corresponds to the 3-dimensional T vector loop. The red vectors indicate the instantaneous velocity of the blue arrows' (i.e. heart vector's) movement. We refer to this quantity as TVV, and it is fundamental to the suggested biomarkers.

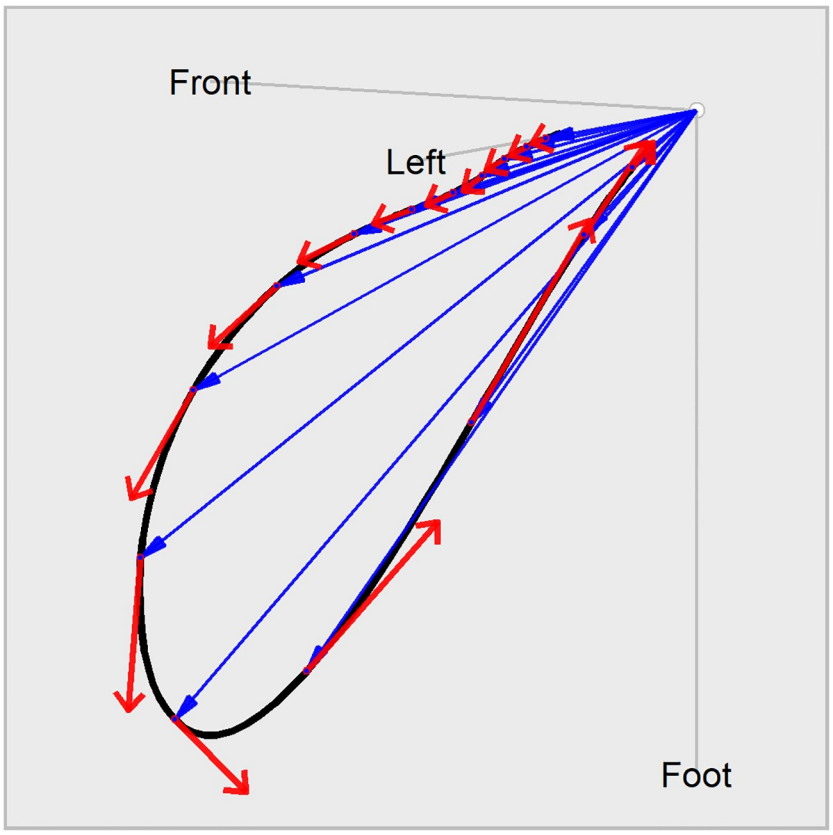

Fig 1. Derivation of the TVV from the T vector loop. Displayed is the time course of the heart vector in 20 ms steps (blue arrows), forming the 3-dimensional T vector loop (black curve). The red arrows indicate the TVV, the velocity at which the heart vector is moving at the given times.

https://doi.org/10.1371/journal.pone.0204712.g001

We estimated the TVV by separately calculating the temporal derivatives $\dot{x}(t)$, $\dot{y}(t)$ and $\dot{z}(t)$ for the three VCG components and calculated its magnitude as $TVV(t) = \sqrt{\dot{x}(t)^2 + \dot{y}(t)^2 + \dot{z}(t)^2}$. We obtained the temporal derivatives by means of a differentiating Savitzky-Golay polynomial smoothing filter (R method sgolayfilt, package *signal*, version 0.7–6) of order 3 and filter length of 31 samples, equivalent to a time window length of 60 msec. The rationale for our choice of filter settings is described in the supporting information S2 Text.

Integration of the TVV over a time interval corresponds to a cumulative summation of all spatio-temporal changes of the T vector trajectory, and yields the length of the T vector trajectory in the given time span. Normalizing the total T vector trajectory length to 1 allows interpreting the time course of the integrated TVV as a distribution function for the trajectory's time course. The X% quantile of this distribution corresponds to the time elapsed until X% of the total T vector trajectory length have been reached. To assess drug effects throughout the entire repolarization phase, we used the 10%, 20%, 30%, 40%, 50%, 60%, 70%, 80%, 90%, and 100% trajectory quantiles as parameters, and named them *Tr*10, *Tr*20, . . ., *Tr*100. For each ECG, we calculated the T vector trajectory quantile *TrX* as the average of the corresponding quantiles of the normal sinus beats.

Since repolarization is known to be strongly affected by heart rate, the trajectory quantile parameters were corrected for heart rate by fitting a linear mixed effects model (R package *lme4*, version 1.1–13) of the form $TrX \sim 1 + RR + (1 + RR|Subject)$ to all drug-free data in

Studies A and B. The heart rate corrected trajectory quantiles were calculated as $TrXc = TrX - \beta^* (RR - 1000)$, where β represents the model's fixed effect slope estimate, and RR the ECG's average beat interval measured in milliseconds. The rationale for our choice of heart rate correction method is described in the supporting information S4 Text.

Fig 2 illustrates derivation of the T vector trajectory quantiles with the ECGs of subject 1017 from Study A under placebo and under quinidine treatment where colors indicate the relative time points. The upper row displays the T vector loops in 3-dimensional space, indicating normal diurnal variation in the placebo column, and quinidine induced T loop morphology changes in addition to circadian effects. With respect to the body orientation, the front direction corresponds to x, left direction to y, and foot direction to the negative z VCG component. Small dots indicate the start of the T vector trajectories, which are 20ms after the J-point. The second row displays the time courses of the T vector strength (TVS), calculated as $TVS(t) = \sqrt{x(t)^2 + y(t)^2 + z(t)^2}$, which would be the basis signals for T_{peak} measurements as applied in the FDA studies A and B (note the flattening and trend toward notching for quinidine). The third row displays the time course of the TVV, and the fourth row the cumulated and normalized TVV over time, which is identical to the relative vector trajectory length at a given time. The horizontal lines denote the 30% and 70% trajectory quantiles. Note that the cumulated TVV curves are nicely aligned with stable relative positions under placebo, but intersect under quinidine. Notably, in the first hours after quinidine dosing corresponding to high quinidine plasma concentrations, the 30% quantiles are decreased, while the 70% quantiles are increased. The time axes in Fig 2 are corrected for heart rate according to Fridericia's formula.

Evaluation of drug effects

The T vector trajectory quantiles TrXc described above are the basis for our evaluation of drug effects on ventricular repolarization. In order to quantify a drug effect, single-delta parameter values were calculated as $\Delta P(t, TR) = P(t, TR) - P(t_0, TR)$, with $P(t, TR)$ as the average parameter value of the replicate ECGs at time t under treatment TR for a given subject, and t_0 as the baseline time point. Subsequently, double-delta parameter values were derived as $\Delta\Delta P(t, Drug) = \Delta P(t, Drug) - \Delta P(t, Placebo)$.

We modeled the dependencies of the T vector trajectory quantile parameters on the drug concentrations by means of the mixed effects models $\Delta\Delta P \sim 0 + C + (0 + C|Subject)$ (for single drugs in Study A) respectively $\Delta\Delta P \sim 0 + C1 + C2 + C1{:}C2 + (0 + (C1 + C2)|Subject)$ (for two drugs in Study B), where $\Delta\Delta P$ is the placebo corrected change from baseline of the parameter P, and C, C1, C2 are the drug concentrations. The zero terms in both models enforce the regression line or plane to intersect with the origin.

The linear mixed effects models were fitted using the R package *lme4*, version 1.1–13. In order to obtain a drug effect quantification, we evaluated the model predictions at fixed drug concentrations which we considered representative for the range of values actually observed. For Study A, we chose the following drug concentrations: dofetilide: 2500 pg/ml, quinidine: 1500 ng/mL, ranolazine: 2000 ng/mL, verapamil: 100 ng/mL. Fig 3 illustrates these values as vertical grey lines in the dose-response diagrams.

For Study B, which included dosing of two compounds, the representative drug concentrations were determined as the geometric mean drug concentration from the afternoon and evening dosage time points where both drugs had been administered (see Table 2). The model prediction's 95% confidence intervals were estimated through a bootstrap simulation with 2000 replicates (R package *pROC*, version 1.10.0).

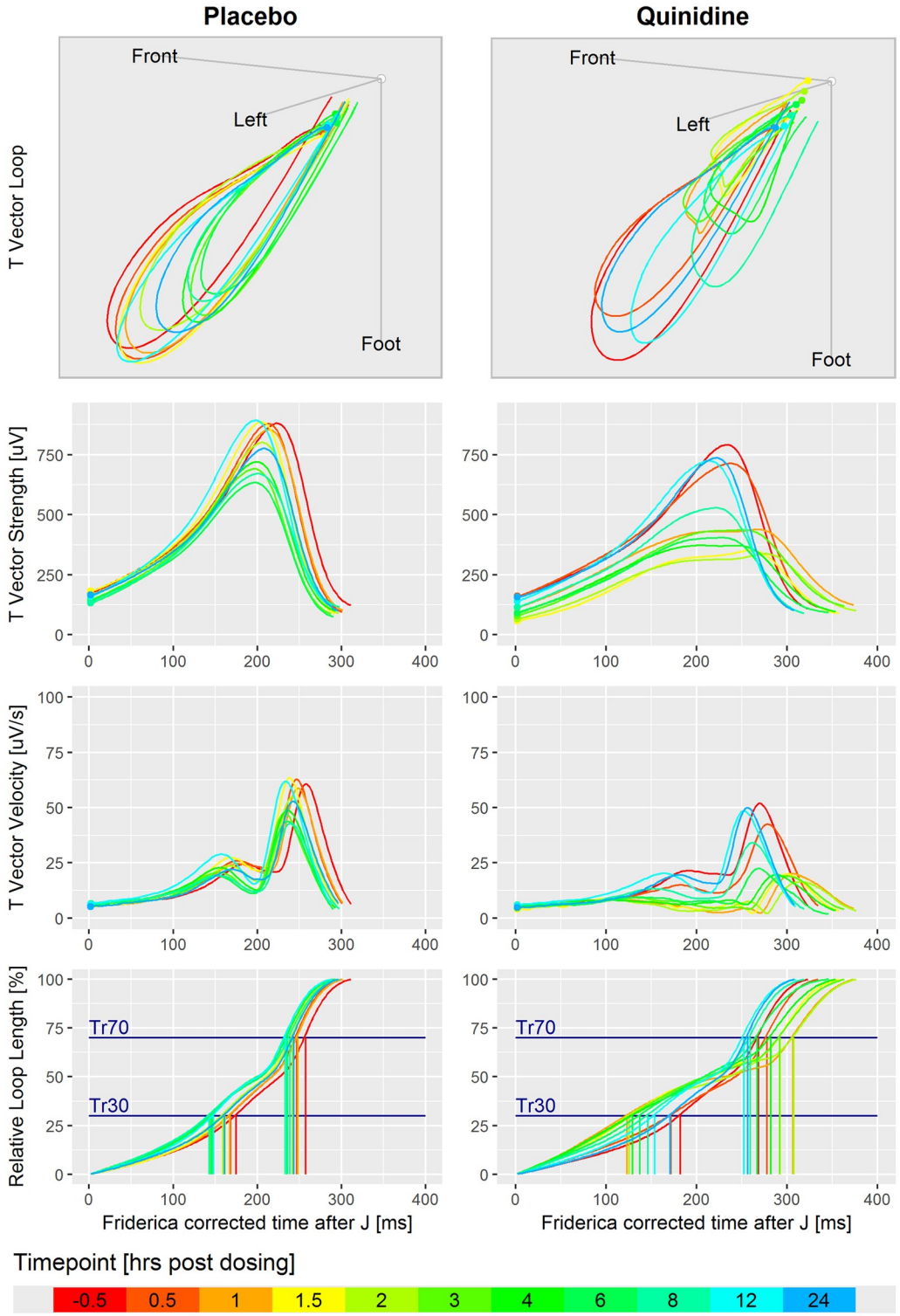

Fig 2. Illustration of the derivation of the TVV and the T vector trajectory quantiles. Displayed are ECGs of subject 1017 in Study A under placebo (left column) and under quinidine treatment (right column). Colors indicate the relative time with respect to dosing. 1st row: T vector loops in the 3-dimensional space. Each loop is the average loop of the normal sinus heartbeats in the first replicate at the given time point. The coordinate system is located in the center of the heart with the axes pointing to the body's front, left side and to the foot. 2nd row: Time courses of the T vector strength. 3rd row: Time courses of the TVV. 4th row: Cumulated and normalized TVV over time, that is the relative loop length reached at a given time, with 30% and 70% trajectory quantiles.

https://doi.org/10.1371/journal.pone.0204712.g002

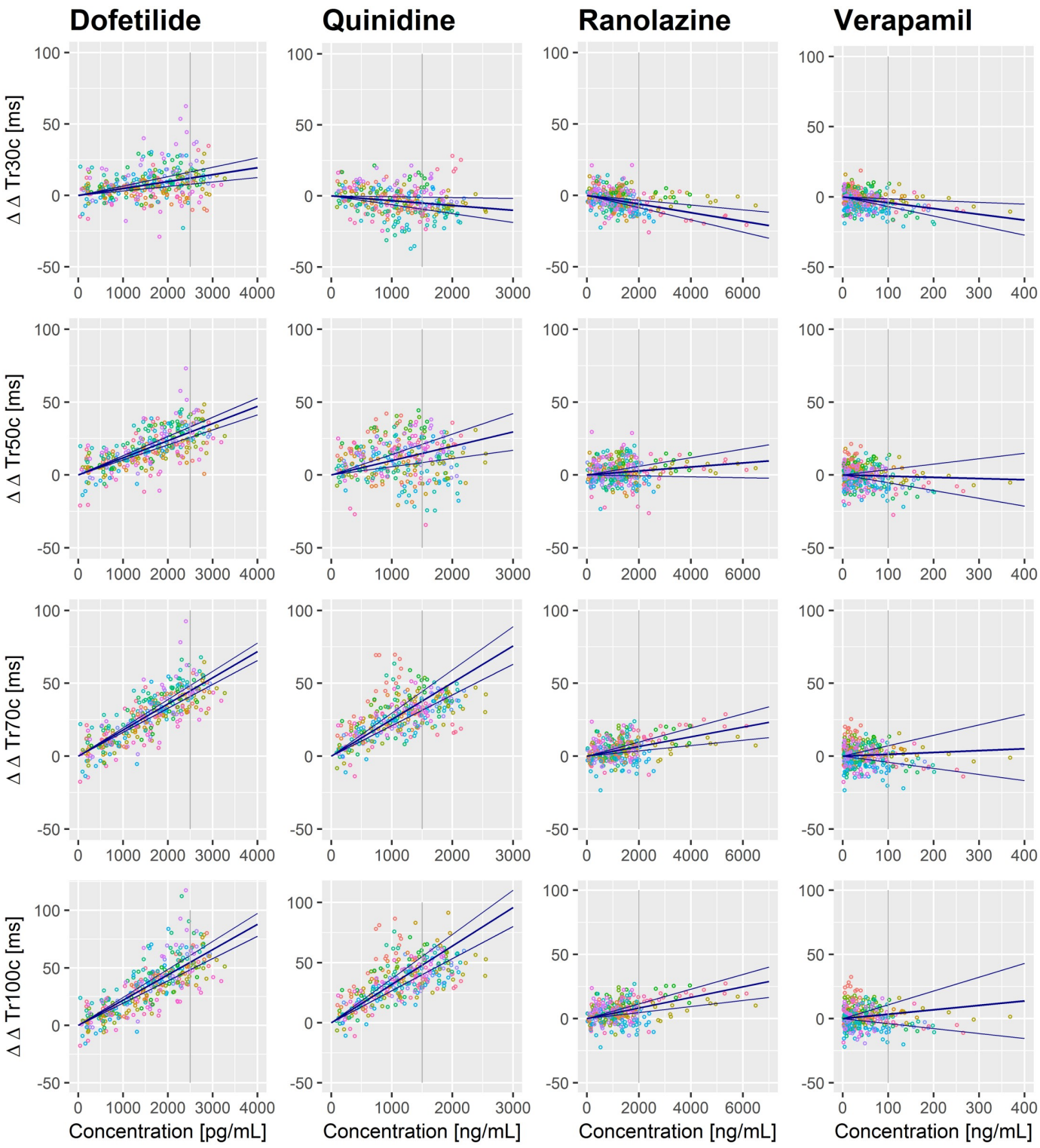

Fig 3. Exposure response in Study A. Effects of dofetilide, quinidine, ranolazine, and verapamil determined as exposure-response relation of the plasma drug concentrations on the double-delta parameters Tr30c, Tr50c, Tr70c, and Tr100c. The blue lines indicate the estimated slope with its 95% confidence interval. The colors of the data points denote individual subjects. The grey vertical lines denote the drug concentrations used for calculating the drug effect profiles in Fig 4.

https://doi.org/10.1371/journal.pone.0204712.g003

Table 2. Representative plasma drug concentrations in Study B.

Drug combination	Drug	Concentration (ng/mL)
Dofetilide + Mexiletine	Dofetilide	1.43
	Mexiletine	1170
Dofetilide + Lidocaine	Dofetilide	1.28
	Lidocaine	1826
Moxifloxacin + Diltiazem	Moxifloxacin	6984
	Diltiazem	71.8

https://doi.org/10.1371/journal.pone.0204712.t002

For assessing the combined effects of mexiletine with dofetilide, we fitted the model to the pooled data from the dofetilide alone treatment period, and the period with combined mexiletine plus dofetilide treatment. The same approach was used for assessing the effects of lidocaine combined with dofetilide. In the assessment of the effect of diltiazem combined with moxifloxacin, we omitted the interaction term $C1{:}C2$ because no data exist for pure diltiazem treatment, and because the regression surfaces for the model including the interaction term revealed implausible distortions. Thus, the predictions of the pure diltiazem effects are model extrapolations and should be interpreted with an appropriate level of caution.

The effects of a drug onto the 10 trajectory quantiles Tr10c to Tr100c (together with the corresponding 95% confidence intervals) constitute what we call a drug effect profile (of Tr*Xc*). A drug effect profile reveals during which phase, and to what extent, a drug delays or accelerates the repolarization process. We derived effect profiles for all drugs in Study A and the various drug combinations in Study B, and examined the effect profile characteristics for their consistency across both studies, and for their plausibility from a physiological perspective.

Classification of pure hERG/iKR current block versus multichannel block

In order to verify the utility of the T vector trajectory quantile parameters in differentiating pure hERG/iKR current block (group I) from multichannel block (group II), we used the data from Study B. To facilitate direct comparisons with the literature, we followed the methods as described in [16]. ECGs from all time points at which selective hERG/iKr current blockers had been dosed (dofetilide and moxifloxacin alone arms in Study B) were considered for group I. ECGs from all time points with additional administration of late sodium blockers (mexiletine with dofetilide and lidocaine with dofetilide arms in Study B) were assigned to group II.

For J-T_{peak}c, QTcF and for each of the 10 trajectory quantiles, we fitted logistic regression classification models $B{\sim}\Delta\Delta P$ where B denotes the block type and $\Delta\Delta P$ the double-delta values of the given parameter (Method glm, R package *stats*, version 3.4.1). Furthermore, we compared the models for the individual parameters with a model consisting of all TrXc parameters $B{\sim}\Delta\Delta Tr10c + \cdots + \Delta\Delta Tr100c$. We assessed the performance in separating group I ECGs from group II ECGs by calculating the area under the receiver-operating curve (AUC). The 95% AUC confidence interval was estimated using a stratified bootstrap technique with 2000 replicates (R package *pROC*, version 1.10.0).

Relation of T vector trajectory quantiles to J-T_{peak} and QT

Since the 100% trajectory quantile Tr100 represents the time interval from J + 20ms to the end of the T wave, we expect that the drug effects as captured by this parameter are similar to those obtained from the QT interval (respectively QTcF). To verify this, we calculated the drug effects of both parameters for Study A and Study B, and compared them visually. (Supporting information S5 Text describes an approach for statistically comparing the drug effects between

QTcF and Tr100c.) Keeping in mind that T_{peak} is typically located roughly in the middle of the J-T_{end} interval, we likewise expect a relation between the J-T_{peak} interval and the central T vector trajectory quantiles. This was addressed by visually comparing the drug effects of published J-T_{peak} data to Tr50 and Tr60 values.

Simulations of ion channel blocks

In order to provide evidence for a physiological interpretation of our results, we calculated action potential waveforms using the O'Hara-Rudy model [26] for human endocardial myocytes with its default parameters. In addition, we simulated a 20% block of the hERG/IKr-Channel, a 90% block of the late sodium (INaL) channel, and a combination of both blocks, by reducing the corresponding model variables of maximum channel conductivity accordingly.

Results

For Study A, Fig 3 displays the drug effects of dofetilide, quinidine, ranolazine, and verapamil in terms of an exposure-response relationship on the (double-delta) 30%, 50%, 70%, and 100% T vector trajectory quantiles. For dofetilide (Fig 3 left column) the slopes in all four graphs are positive. The remaining three compounds show a negative slope for Tr30c (Fig 3, row 1, columns 2–4). Fig 4 displays the effect profiles of all Tr*X*c parameters using representative drug concentrations as described in section 3.4 and indicated as vertical grey lines in Fig 3. Please note that negative effect profile values relate to negative slopes in the exposure-response relation, and positive values correspond to positive slopes. Drug effects on the 10% quantile were negative for all four drugs. Dofetilide displayed a continuously increasing effect profile up to the 100% quantile. The quinidine effect profile was negative up to the 30% quantile with a stronger increase in the middle phase, and slightly reduced growth in the later repolarization phase. The ranolazine effect profile was negative up to the 40% quantile, increased in the mid repolarization phase and stayed close to constant till end of repolarization. Verapamil's effect

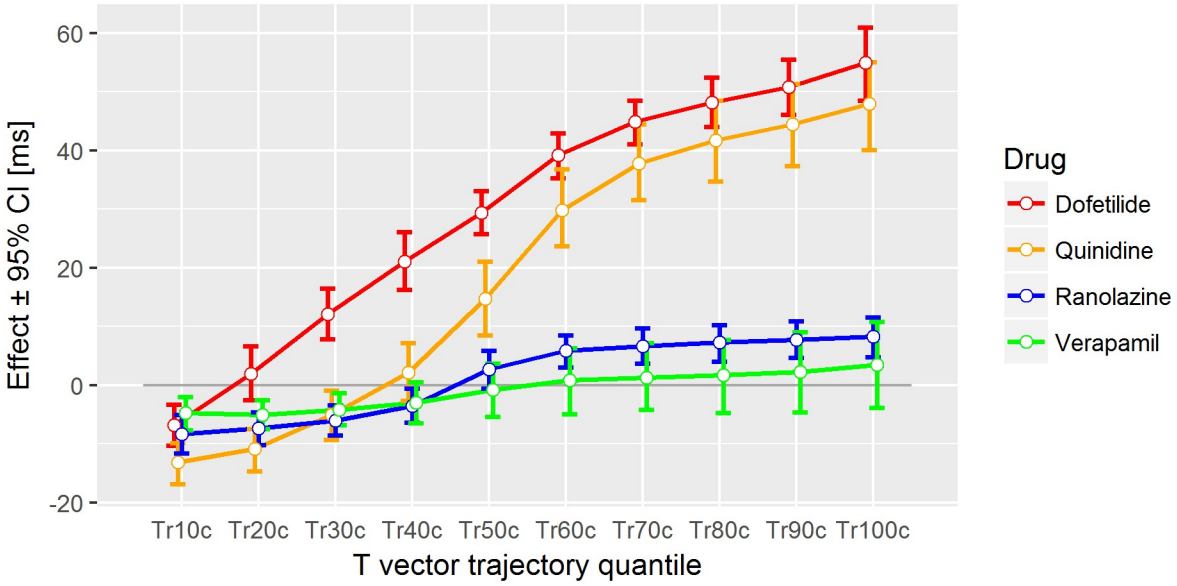

Fig 4. Drug effect profiles in Study A. The effect on the y-axis denotes the placebo-corrected changes from baseline of the T vector trajectory quantiles in milliseconds (corrected for heart rate) with their 95% confidence intervals at the following drug concentrations: dofetilide: 2500 pg/mL, quinidine: 1500 ng/mL, ranolazine: 2000 ng/mL, verapamil: 100 ng/mL.

https://doi.org/10.1371/journal.pone.0204712.g004

profile was slightly negative up to the 40% quantile and stayed close to zero up to the 100% quantile.

For Study B, the effect profiles for the heart rate corrected T vector trajectory quantiles of the various drug combinations are displayed in Fig 5. The drug concentrations used for calculating the drug effect profiles are listed in Table 2. The effect profiles of pure mexiletine and pure lidocaine were very similar in shape, showing a close to zero effect for the 10% quantile, a continuous decreased effect profile up to the 40% quantile, and keeping the negative effect up to the 100% quantile, where mexiletine had a more pronounced negative effect value than lidocaine. The effect profile of pure dofetilide was very similar in shape to the effect profile in Study A. The combinations of mexiletine plus dofetilide and of lidocaine plus dofetilide generated sigmoid-like effect profiles, which were similar in shape to the ranolazine effect profile in Study A: The 10% to 40% quantiles were negative with a transition to positive in the mid-repolarization phase, and a slightly increasing trend up to the 100% quantiles.

The effect profile of moxifloxacin alone was completely positive with constantly increasing values from the 10% to the 100% quantile. Combining moxifloxacin with diltiazem slightly increased the late-repolarization related quantiles, and slightly decreased the early-repolarization related quantiles.

Figs 6 and 7 demonstrate that the double-delta changes of the 100% T vector trajectory quantiles are comparable in size and precision to the double-delta changes of QTcF for all treatments. (For a statistical test comparing drug effects on QTcF and Tr100c see Supplement S5 Text). The highest correlation with the published J-T_{peak} data was observed for the 50% and 60% T vector trajectory quantiles. This also holds for the majority of the cases under treatment (Figs 6 and 7). Notably, most confidence intervals for J-T_{peak}c were larger than those of the 50% and 60% T vector trajectory quantiles. (For a comparison of the distributions of QTcF, J-T_{peak}c and the TrXc parameters in drug-free ECGs see Supplement S6 Text).

The AUC values for separating selective hERG/iKr current block versus multichannel block with late sodium current inhibition (Study B) are displayed in Figs 8 and 9. The largest AUC value for a single parameter was observed for the 40% T vector trajectory quantile with 0.90, CI = [0.88 to 0.92] (Fig 8). Combining all 10% step quantile parameters increased the AUC value to 0.94, CI = [0.92 to 0.96] (Fig 9). The AUC value for J-T_{peak}c (published data) was 0.81, CI = [0.78 to 0.84], and the AUC value for QTcF using the eECG/ABBIOS generated annotations was 0.73, CI = [0.69 to 0.77].

The results of the simulations based on the O'Hara-Rudy model are shown in Fig 10. They demonstrate that blocking the late sodium ion channels causes a steeper descent of the AP in particular in phase 2 (Fig 10 emerald curve vs. red curve) resulting in accelerated repolarization. In contrast, a block of the hERG/IKr current delays repolarization by reducing the downslope of the action potential in both, phase 2 and phase 3 (Fig 10 green curve vs. red curve). The combination of both blocks (Fig 10 violet curve) shows that their oppositional effects largely compensate in phase 2, whereas in phase 3 the effect of the hERG/IKr block prevails.

Discussion

In this study, we present and evaluate heart rate corrected quantiles of the heart's dipole vector trajectory along the 3-dimensional T vector loop as a new set of ECG biomarkers for assessing drug effects on the repolarization process. We define the *X*% T vector trajectory quantile Tr*X* as the time after the J point when *X*% of the total T vector trajectory length has been reached. From a conceptual point of view, the major advancement entailed by TVV analysis is its capability to quantify drug effects as delays or accelerations quasi-continuously over the entire time range of repolarization. Thus, in contrast to QTc, drug effects can be associated with the

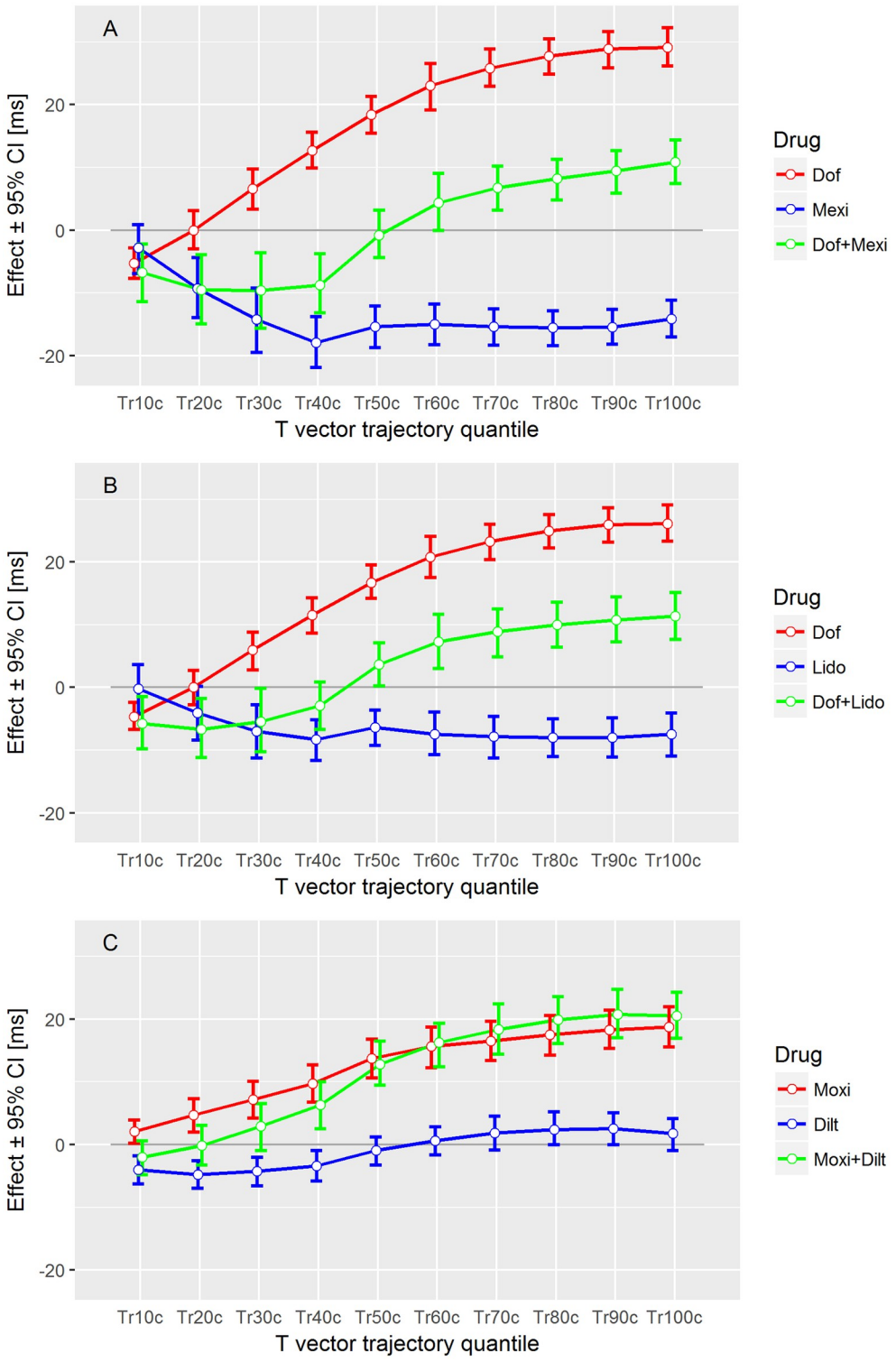

Fig 5. Drug effect profiles in Study B. The effect on the y-axis denotes the placebo-corrected changes from baseline of the T vector trajectory quantiles in milliseconds (corrected for heart rate) with their 95% confidence intervals at the drug concentrations as given in Table 2.

https://doi.org/10.1371/journal.pone.0204712.g005

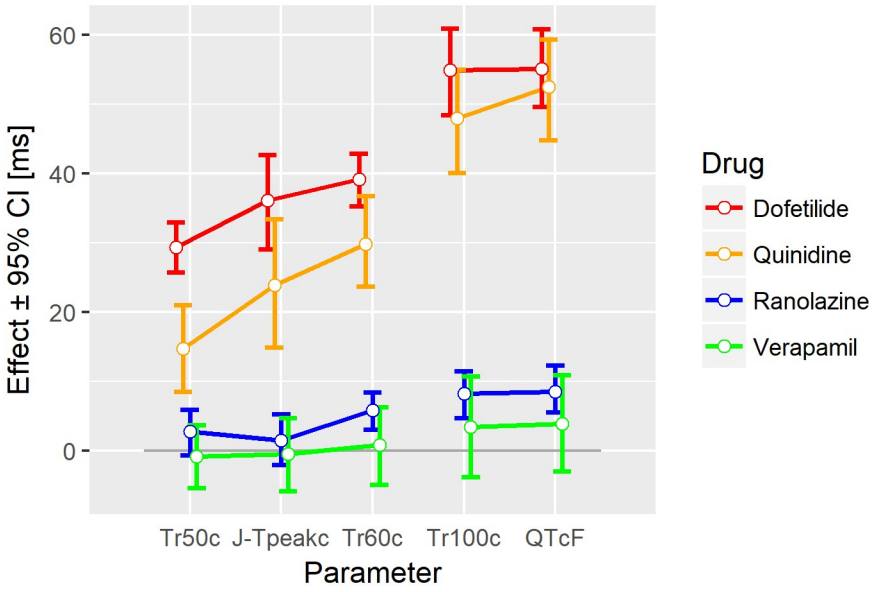

Fig 6. Drug effects on selected parameters in Study A. The drug effects on J-T_{peak}c are about between the effects of the 50% and 60% T vector trajectory quantiles (Tr50c and Tr60c) but have larger confidence intervals. The effects on the 100% T vector trajectory quantile (Tr100c) are comparable to the effects on QTcF.

https://doi.org/10.1371/journal.pone.0204712.g006

relative phase of repolarization. This additional level of detail unveils that blocking of inward ion currents which maintain the plateau phase 2 of the cardiac action potential (late sodium and calcium) causes acceleration of the cellular repolarization process mainly during earlier repolarization. In contrast, blocking of the hERG/iKr current increasingly delays repolarization over its entire course. The method's potential is highlighted by the fact that it clearly outperforms the current state of the art in separating multi-ion channel block from pure hERG/IKr block. But we are confident that the TVV approach can provide still more sophisticated information. We propose that systematic analysis of the TrX effect profile permits temporal disentanglement of superimposed multi-ion channel activity. It reveals information about the relative effect size of ion current blockade at the cellular level, and this information can be assessed from the surface ECG. We see an important future role for TVV analysis in characterizing a drug's effects on ion channels in vivo and in the assessment of its pro-arrhythmic potential.

In the following paragraphs, we discuss and substantiate these high-level findings and propositions in detail. We first present our hypothesis on how TrX quantiles can be interpreted and how we associate them with the underlying cellular physiology, and then motivate this interpretation from our results.

Interpretation of T vector trajectory quantiles

The *X*% T vector trajectory quantile Tr*X* denotes the time when *X*% of the total T vector trajectory length has been reached. Arriving earlier at a particular point on the T vector trajectory (as compared to placebo) means that the repolarization process is accelerated in the corresponding phase of repolarization. Hence, the dose-response curve of this placebo-corrected change from baseline quantile shows a negative slope, and its effect profile value is negative. In contrast, an increase in the time required to reach a particular point on the T vector trajectory indicates a delay of the repolarization process, and is associated with a positive slope in the dose-response curve and a positive value in the effect profile. The magnitude of an effect

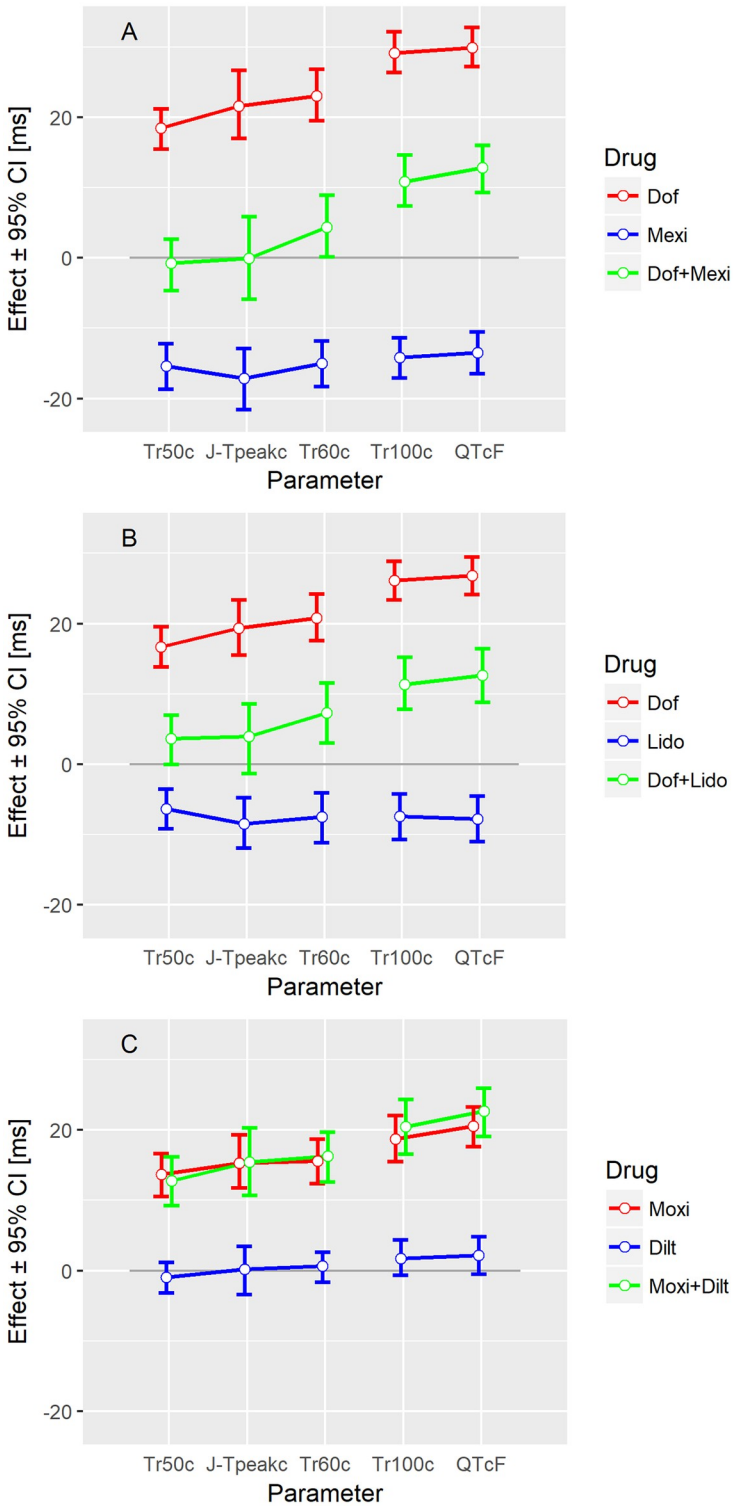

Fig 7. Drug effects on selected parameters in Study B. The drug effects on J-T_{peak}c are between the effects of the 50% and 60% T vector trajectory quantiles (Tr50c and Tr60c) but have larger confidence intervals. The effects on the 100% T vector trajectory quantile (Tr100c) are comparable to the effects on QTcF.

https://doi.org/10.1371/journal.pone.0204712.g007

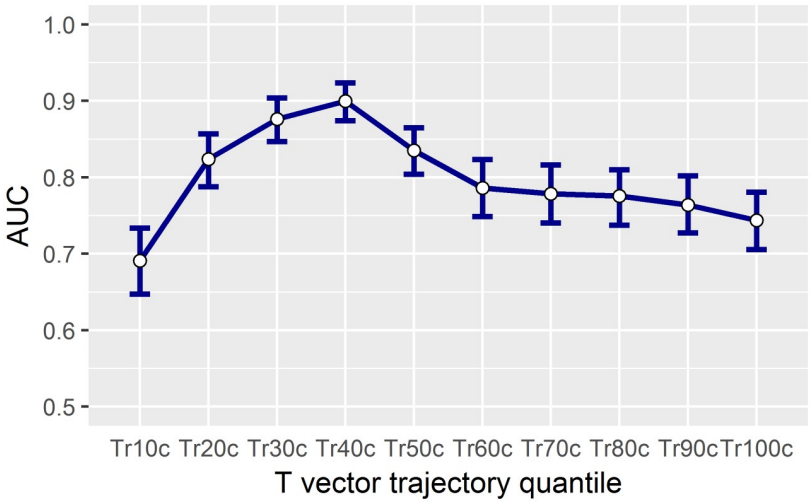

Fig 8. Performance of separating pure hERG/iKr current block from multichannel block based on individual T vector trajectory quantiles. Separation performance between group I and group II (see section 3.5) is measured by the area under the receiver-operating curve (AUC) with its 95% confidence intervals. The T vector trajectory quantiles Tr10c to Tr100c are corrected for heart rate. Best separation is observed for the 40% quantile Tr40c.

https://doi.org/10.1371/journal.pone.0204712.g008

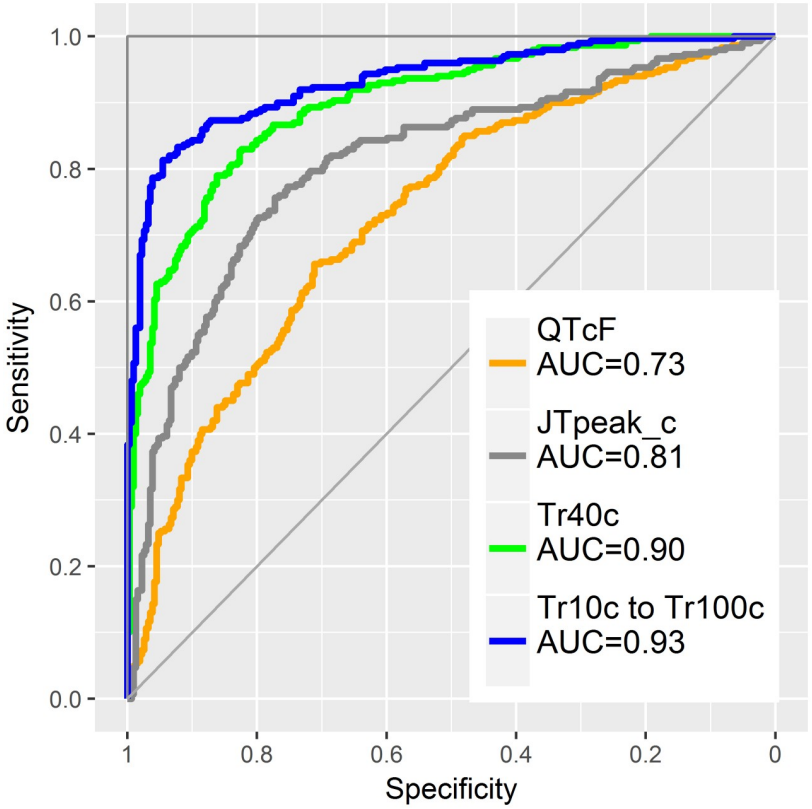

Fig 9. Classification of pure hERG/iKr current block versus multichannel block in logistic regression models. The separation performance (AUC) of the heart rate corrected T vector trajectory quantile Tr40c (green curve) and the combined 10 Tr*X* quantiles (blue curve) are compared to QTcF (orange curve) and to published [16] J-T_{peak}c data (grey curve).

https://doi.org/10.1371/journal.pone.0204712.g009

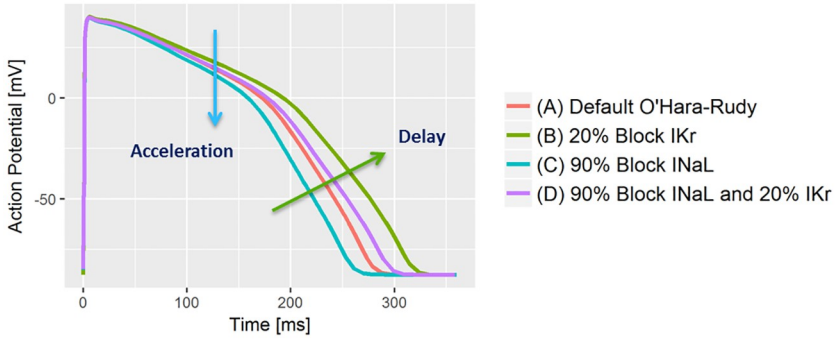

Fig 10. Simulation of blocking of the late sodium (INaL) and the hERG/IKr currents in the O'Hara-Rudy model using the endocardial cell type. Blocking INaL accelerates the repolarization process by increasing the downslope in AP phase 2. Blocking IKr decreases the downslope of the AP in both, phase 2 and phase 3, resulting in delayed repolarization. In simultaneous blocking, the effects compensate in phase 2 but a delay in phase 3 is still evident.

https://doi.org/10.1371/journal.pone.0204712.g010

profile value reflects the effect size, i.e. the extent of acceleration or delay, with respect to a given drug concentration.

We propose a link between cellular repolarization changes resulting from blockade of single and multiple ionic currents and the observed Tr*X* effect profiles as illustrated in Fig 10: Inward sodium and calcium ion currents are predominantly active during earlier repolarization, and both contribute to the maintenance of the action potential's plateau phase. In our simulation based on the O'Hara-Rudy model [26], blocking the late sodium ion channels causes a steeper descent of the AP in phase 2 (Fig 10 emerald curve vs. red curve). This represents an acceleration of the repolarization process and earlier restitution of the resting potential. Phase 3 of the AP appears only marginally affected by pure sodium ion channel block (Fig 10) as the red and emerald curve run almost in parallel in phase 3, i.e. their downslopes have comparable magnitude.

We expect that faster intracellular action potential changes are reflected in higher speed of progression along the T vector trajectory. If sodium-block related acceleration predominantly happens in phase 2 of the AP, it should increase the TVV in the initial part of the T vector trajectory. Hence, the corresponding lower T vector trajectory quantiles will be reached earlier, resulting in negative effect profile values for the lower quantiles. This phenomenon is observable in all effect profiles of the late sodium current blockers mexiletine (Fig 5A blue line) and lidocaine (Fig 5B blue line), where the lower quantiles Tr10c to Tr40c are continuously decreased. The accumulated level of time lead is maintained over the second part of repolarization with Tr50c to Tr100c remaining at a negative effect profile level comparable to that of Tr40c. This is in accordance with the limited effect of pure sodium ion channel block onto phase 3 of the AP in our simulation (Fig 10). Overall, this indicates that the slight QTcF shortening effect of these two drugs is mainly caused by an acceleration of early repolarization, which then is largely maintained.

Fig 10 also shows that pure hERG/iKr current block causes a reduction of the downslope in the AP in both phase 2 and phase 3 (green curve vs. red curve), corresponding to a delay which affects all parts of the repolarization process. The effect profiles of both pure hERG/iKr current blockers dofetilide (red curves in Figs 4, 5A and 5B) and moxifloxacin (red curve in Fig 5C), consistently reflect this. They show a continuously increasing delay, indicating that the QT prolongation caused by these drugs are effective over the entire course of repolarization.

A combined block of sodium and hERG/iKr currents results in a superposition of the single effects in the AP waveform (Fig 10 violet curve). The reduced downslope of pure hERG/iKr

current block (green curve) is largely compensated for by the additional sodium channel block in phase 2 (Fig 10 violet curve vs. red curve), but is still evident in phase 3 (note the reduced downslope of the violet curve versus the red one). The effect profiles of the corresponding drug combinations dofetilide + mexiletine (Fig 5A, green curve) and dofetilide + lidocaine (Fig 5B, green curve) are well in line with this. Their sigmoid shape indicates a slight, but largely balanced, acceleration of the repolarization process in the early T vector trajectory quantiles Tr10c to Tr40c (associated with the effect of the sodium ion channel block in AP phase 2 and the counteracting hERG/iKr current block), which then becomes increasingly delayed by the preponderance of the hERG/iKr current block effect in AP phase 3.

In the case of mexiletine, the combined effect profile (Fig 5A, green curve) is an approximately linear combination of the pure drug effect profiles (Fig 5A, red curve and blue curve). For lidocaine, the effect profile of the drug combination (Fig 5B, green curve) is slightly more depressed compared to the pure lidocaine effect alone (Fig 5B, blue curve). This is owing to a significant contribution of the interaction term $C1 * C2$ in the mixed effects model to all T vector trajectory quantile parameters.

The presented interpretation is further supported by the effect profiles of drugs, which simultaneously affect multiple ion channels. Ranolazine blocks both the hERG/iKr and the late sodium currents, and shows the same sigmoid-shaped effect profile (Fig 4 blue curve) observed for the combinations of the individual channel blockers (Fig 5A and 5B green curves).

Verapamil predominantly blocks the L-type calcium ion channel, mainly affecting AP phase 2, i.e. early repolarization, and to a lesser extent the hERG/iKr current. In line with this, its effect profile (Fig 4, green curve) indicates a slight but significant acceleration of the heart's electrical activity in the early repolarization, which is compensated for during late repolarization but does not result in significant prolongation of the overall repolarization duration, measured by the QTcF interval.

The effect profile of quinidine (Fig 4, orange curve) as a strong hERG/iKr current blocking drug as well as calcium and sodium current blocking agent indicates significant acceleration in the early repolarization phase and a strong delay in the mid and late repolarization phases. On the other hand, the effect profile of dofetilide (Fig 4, red curve) as a pure hERG/iKr current blocker indicates (with exception of Tr10c) continuously increasing delay throughout repolarization.

As reported in [15], the combination of diltiazem with moxifloxacin in the evening dose did unexpectedly slightly increase QTcF, despite a slightly reduced moxifloxacin plasma concentration compared to the afternoon (pure moxifloxacin). Our analysis shows that diltiazem slightly accelerates repolarization in the early phase (Fig 5C, green curve for Tr10c to Tr40c), which may be due to its calcium ion channel block. However, diltiazem delays the later repolarization phase, finally increasing the repolarization delay induced by moxifloxacin. Note that the pure diltiazem effect profile (Fig 5C, blue curve) was calculated as an extrapolation of the mixed effects model and should be interpreted with care.

The body surface potentials observed through the T vector loop are results of a complex integration of cellular action potentials from different myocardial cell types (endocardial, epicardial, M cells) with different activation times, modulated among others by spatial gradients in ion channel expression. Thus, the proposed link between cellular repolarization and TrX effect profiles should be taken as a reasonable and plausible attempt to explain our clinical findings rather than a rigorous mechanistic proof. Moreover, the available number of drugs was limited and should certainly be expanded in future. But in summary, our current results support the presented interpretation and suggest that the concept of the TrX effect profile constitutes an electrocardiographic fingerprint of a drug's impact on repolarization. It reveals the

presence, extent and relative phase of drug-induced alterations in the timing (delays or accelerations) of the ventricular repolarization process. Tr*X*c effect profiles extend repolarization assessment beyond QTc and the T_{peak} fiducial point to a quasi-continuous view onto the entire repolarization process.

Differentiation of pure hERG/iKr current block versus multichannel block

Our results confirm that T vector trajectory quantiles enhance differentiation of multichannel block from pure hERG/iKr current block. In our data, pure hERG/iKr current block consistently manifests as an increasing delay of repolarization with a slightly higher slope between Tr10c to Tr60c compared to Tr60c to Tr100c (Figs 4 and 5, red lines). The presence of additional effective ion channel blocks is revealed by deviations from this profile. According to the previous discussion, the effect of late sodium ion channel block should be particularly evident during phase 2 of the AP. The finding that the "early" T vector trajectory quantiles Tr20c, Tr30c and Tr40c demonstrate the best separation (Fig 8), and that Tr40c is most effective among all T vector trajectory quantiles to identify additional late sodium block (Fig 8) is well in line with this assumption. Note that the performance of the 40% quantile of the T vector trajectoryTr40c, reaching an AUC of 0.9 (Fig 9), is significantly higher than that provided by J-T_{peak} (0.81) representing the best previously published ECG biomarker for that purpose [15, 16]. The potential of the effect profile in identifying multi-ion channel effects is highlighted by a further increase in performance observed when the entire profile is used in the classification process (Fig 9, AUC 0.94). Well aware of the danger of overfitting a 10-parameter-model to a data set of limited size, we take this improvement only as an additional hint that requires prospective validation.

Relation of Tr*X* to QT and J-T_{peak}

Since QTcF and Tr100c just differ in the starting point (Q versus J+20ms) and in a slightly different correction formula for heart rate, it is not surprising that their effects are largely comparable in magnitude and precision. The slight differences may arise from drug effects on QRS duration, from the different heart rate correction methods for QTcF and Tr100c, or from systematic differences of our algorithms' robustness with respect to identification of the J point and the onset of Q.

ECG effects described by the Tr*X* parameters are in line with effects described by parameters, which are derived from the T_{peak} fiducial point: Pure hERG/iKr current blocking drugs delay repolarization through the entire repolarization process, indicated by continuously increasing parameters Tr10 to Tr100. Drugs or drug combinations that additionally block late sodium or calcium ion currents shorten the parameters Tr10 to Tr40. Accordingly, pure hERG/iKr current blocking drugs prolong both the J-T_{peak} and the T_{peak}-T_{end} intervals, while J-T_{peak} tends to be shortened by multichannel blocking drugs [27]. However, declaring T_{peak} as cutting point between early and late repolarization is questionable [28], and there is no generally accepted physiologic reason for choosing the T_{peak} to subdivide the repolarization interval for assessment of pro-arrhythmic effects [29]. It has recently been challenged whether a lack of J-T_{peak} prolongation can reliably differentiate between safe and proarrhythmic QT_{end} prolongation [30].

Using a simplified model of VCG generation, we would expect T_{peak} to represent the instant in time when the largest spatial gradient of intracellular potentials exists, i.e. a moment of maximum heterogeneity of the action potentials in all heart cells. From our new parameters, the Tr50c and Tr60c quantiles correspond most closely with J-T_{peak}c. For the majority of drugs,

the effect size of J-T_{peak}c is located between that of Tr50c and Tr60c (Figs 6 and 7, lines on left side).

The clear trend for narrower confidence intervals of Tr50c and Tr60c, compared to J-T_{peak}c (Figs 6 and 7, lines on left hand side), suggests that the determination of the T vector trajectory quantiles is more robust than that of the T_{peak} position. This is not surprising in view of the demonstrable changes of T wave morphology induced by drugs, including severe flattening or notching. In such a setting, small alterations of the intracellular potential distribution may cause significant dislocation of the T_{peak} position, increasing J-T_{peak} parameter variability. We attribute the robustness of the T vector trajectory quantiles Tr*X* to their unique identifiability even in the presence of significant changes in T wave / T loop morphology and consider this an advantage compared to J-T_{peak}.

Another conceptual difference between J-T_{peak} and the Tr*X* parameters is that the J-T_{peak} determination is purely based on the T vector's magnitude, while the Tr*X* parameters capture changes of both the magnitude and the direction of the T vector progression. Since directional changes of the T vector trajectory reflect changes of the distribution of electrical activities in the whole heart, this information may contribute to the performance improvement in differentiating multi-channel blockade.

Conclusion

The T vector trajectory quantiles and the related effect profiles extend the discrete ECG characteristics T_{peak} and QT to a quasi-continuous view on the repolarization process. Linking the effect size and direction to the relative phase of repolarization, they allow more detailed description of drug effects on the various ionic currents, and enable better differentiation of single versus multichannel block than the currently best biomarker for this purpose, J-T_{peak}.

The TVV based approach enhances characterization of drug effects on cardiac myocyte ion channels, and improves the in-vivo assessment of the proarrhythmic risk of drugs from the surface ECG. If the proposed functional linkage between drug effects on cellular levels and the TVV measured on the ECG can be prospectively confirmed on a larger set of subjects and drugs, the suggested approach will constitute an important milestone in the alignment of information retrieved in the four components of the Comprehensive in vitro Proarrhythmia Assay (CiPA).

We intend to analyze the data of a third FDA-sponsored study, which has recently been released to the public (ClinicalTrials.gov, NCT03070470, [31]) as a first step towards this goal.

Supporting information

S1 Text. Rationale for choosing the Dower transformation.
(PDF)

S2 Text. Rationale for filter settings.
(PDF)

S3 Text. Agreement of QTcF data.
(PDF)

S4 Text. Rationale for the heart rate correction approach.
(PDF)

S5 Text. Comparison of the drug effects between QTcF and Tr100c.
(PDF)

S6 Text. Distribution of QTcF, J-T_{peak}c and TrXc.
(PDF)

Acknowledgments

AbbVie did review this publication and provide approval for its submission for publication, but did not contribute to the interpretation of data or writing of this publication.

The authors deeply thank and acknowledge the FDA for conducting the Study A and B, and for making the data available to the scientific community.

Author Contributions

Conceptualization: Werner Bystricky, Christoph Maier.

Data curation: Gary Gintant, Dennis Bergau, Kent Kamradt, Patrick Welsh, David Carter.

Formal analysis: Werner Bystricky, Christoph Maier.

Investigation: Werner Bystricky, Christoph Maier.

Methodology: Werner Bystricky, Christoph Maier.

Software: Werner Bystricky, Christoph Maier.

Supervision: Gary Gintant, Dennis Bergau, Kent Kamradt, Patrick Welsh, David Carter.

Visualization: Werner Bystricky, Christoph Maier.

Writing – original draft: Werner Bystricky, Christoph Maier.

Writing – review & editing: Gary Gintant, Dennis Bergau, Kent Kamradt, Patrick Welsh, David Carter.

References

1. ICH. The clinical evaluation of qt/qtc interval prolongation and proarrhythmic potential for non-antiarrhythmic drugs; 2005. http://www.ich.org/fileadmin/Public_Web_Site/ICH_Products/Guidelines/Efficacy/E14/E14_Guideline.pdf.
2. Couderc JP. Measurement and regulation of cardiac ventricular repolarization: from the QT interval to repolarization morphology. Philosophical Transactions Series A, Mathematical, Physical, and Engineering Sciences. 2009 Apr; 367:1283–1299. https://doi.org/10.1098/rsta.2008.0284 PMID: 19324709
3. Brennan TP, Tarassenko L. Review of T-wave morphology-based biomarkers of ventricular repolarisation using the surface electrocardiogram. Biomedical Signal Processing and Control. 2012; 7:278–284.
4. Gupta P, Patel C, Patel H, Narayanaswamy S, Malhotra B, Green JT, et al. T(p-e)/QT ratio as an index of arrhythmogenesis. Journal of Electrocardiology. 2008; 41:567–574. https://doi.org/10.1016/j.jelectrocard.2008.07.016 PMID: 18790499
5. Jie X, Rodriguez B, Pueyo E. A new ECG biomarker for drug toxicity: A combined signal processing and computational modeling study. In: Proc. Annual Int. Conf. of the IEEE Engineering in Medicine and Biology; 2010. p. 2565–2568.
6. Acar B, Yi G, Hnatkova K, Malik M. Spatial, temporal and wavefront direction characteristics of 12-lead T-wave morphology. Medical & Biological Engineering & Computing. 1999 Sep; 37:574–584.
7. Draisma HHM, Schalij MJ, van der Wall EE, Swenne CA. Elucidation of the spatial ventricular gradient and its link with dispersion of repolarization. Heart Rhythm. 2006 Sep; 3:1092–1099. https://doi.org/10.1016/j.hrthm.2006.05.025 PMID: 16945809
8. Couderc JP, McNitt S, Hyrien O, Vaglio M, Xia X, Polonsky S, et al. Improving the detection of subtle I(Kr)-inhibition: assessing electrocardiographic abnormalities of repolarization induced by moxifloxacin. Drug Safety. 2008; 31:249–260. https://doi.org/10.2165/00002018-200831030-00006 PMID: 18302449
9. Andersen MP, Xue JQ, Graff C, Hardahl TB, Toft E, Kanters JK, et al. A robust method for quantification of IKr-related T-wave morphology abnormalities. In: Proc. Computers in Cardiology; 2007. p. 341–344.

10. Graff C, Andersen MP, Xue JQ, Hardahl TB, Kanters JK, Toft E, et al. Identifying drug-induced repolarization abnormalities from distinct ECG patterns in congenital long QT syndrome: a study of sotalol effects on T-wave morphology. Drug Safety. 2009; 32:599–611. https://doi.org/10.2165/00002018-200932070-00006 PMID: 19530746
11. Malik M. Drug-induced changes in the T-wave morphology. Drug Safety. 2009; 32:613–617. https://doi.org/10.2165/00002018-200932070-00007 PMID: 19530747
12. Sager PT, Gintant G, Turner JR, Pettit S, Stockbridge N. Rechanneling the cardiac proarrhythmia safety paradigm: a meeting report from the Cardiac Safety Research Consortium. American Heart Journal. 2014 Mar; 167:292–300. https://doi.org/10.1016/j.ahj.2013.11.004 PMID: 24576511
13. Johannesen L, Vicente J, Mason JW, Sanabria C, Waite-Labott K, Hong M, et al. Differentiating drug-induced multichannel block on the electrocardiogram: randomized study of dofetilide, quinidine, ranolazine, and verapamil. Clinical Pharmacology and Therapeutics. 2014 Nov; 96:549–558. https://doi.org/10.1038/clpt.2014.155 PMID: 25054430
14. Vicente J, Johannesen L, Mason JW, Crumb WJ, Pueyo E, Stockbridge N, et al. Comprehensive T wave morphology assessment in a randomized clinical study of dofetilide, quinidine, ranolazine, and verapamil. Journal of the American Heart Association. 2015 Apr; 4.
15. Johannesen L, Vicente J, Mason JW, Erato C, Sanabria C, Waite-Labott K, et al. Late sodium current block for drug-induced long QT syndrome: Results from a prospective clinical trial. Clinical Pharmacology and Therapeutics. 2016 Feb; 99:214–223. https://doi.org/10.1002/cpt.205 PMID: 26259627
16. Vicente J, Johannesen L, Hosseini M, Mason JW, Sager PT, Pueyo E, et al. Electrocardiographic Biomarkers for Detection of Drug-Induced Late Sodium Current Block. PloS one. 2016; 11:e0163619. https://doi.org/10.1371/journal.pone.0163619 PMID: 28036334
17. Colatsky T, Fermini B, Gintant G, Pierson JB, Sager P, Sekino Y, et al. The Comprehensive in Vitro Proarrhythmia Assay (CiPA) initiative—Update on progress. Journal of pharmacological and toxicological methods. 2016; 81:15–20. https://doi.org/10.1016/j.vascn.2016.06.002 PMID: 27282641
18. Badilini F, Libretti G, Vaglio M. Automated JTpeak analysis by BRAVO. Journal of electrocardiology. 2017; 50:752–757. https://doi.org/10.1016/j.jelectrocard.2017.07.010 PMID: 28826858
19. Goldberger AL, Amaral LA, Glass L, Hausdorff JM, Ivanov PC, Mark RG, et al. PhysioBank, PhysioToolkit, and PhysioNet: components of a new research resource for complex physiologic signals. Circulation. 2000 Jun; 101:E215–E220. https://doi.org/10.1161/01.cir.101.23.e215 PMID: 10851218
20. ECGRDVQ. ECG Effects of Ranolazine, Dofetilide, Verapamil, and Quinidine in Healthy Subjects; 2016. https://www.physionet.org/physiobank/database/ecgrdvq/.
21. ECGDMMLD. ECG effects of Dofetilide, Moxifloxacin, Dofetilide+Mexiletine, Dofetilide+Lidocaine and Moxifloxacin+Diltiazem in Healthy Subjects; 2016. https://www.physionet.org/physiobank/database/ecgdmmld/.
22. Fridericia LS. The duration of systole in an electrocardiogram in normal humans and in patients with heart disease. 1920. Annals of Noninvasive Electrocardiology. 2003 Oct; 8:343–351. PMID: 14516292
23. Meyer CR, Keiser HN. Electrocardiogram baseline noise estimation and removal using cubic splines and state-space computation techniques. Computers and biomedical research, an international journal. 1977 Oct; 10:459–470. PMID: 923219
24. R Core Team. R: A Language and Environment for Statistical Computing. Vienna, Austria; 2017. https://www.R-project.org/.
25. Dower GE, Machado HB, Osborne JA. On deriving the electrocardiogram from vectoradiographic leads. Clinical Cardiology. 1980 Apr; 3:87–95. PMID: 6993081
26. O'Hara T, VirÃ¡g L, VarrÃ³ A, Rudy Y. Simulation of the undiseased human cardiac ventricular action potential: model formulation and experimental validation. PLoS Computational Biology. 2011 May; 7: e1002061. https://doi.org/10.1371/journal.pcbi.1002061 PMID: 21637795
27. Vicente J, Zusterzeel R, Johannesen L, Mason J, Sager P, Patel V, et al. Mechanistic Model-Informed Proarrhythmic Risk Assessment of Drugs: Review of the "CiPA" Initiative and Design of a Prospective Clinical Validation Study. Clinical Pharmacology and Therapeutics. 2018 Jan; 103:54–66. https://doi.org/10.1002/cpt.896 PMID: 28986934
28. Bhuiyan TA, Graff C, Kanters JK, Nielsen J, Melgaard J, Matz J, et al. The T-peak-T-end interval as a marker of repolarization abnormality: a comparison with the QT interval for five different drugs. Clinical Drug Investigation. 2015 Nov; 35:717–724. https://doi.org/10.1007/s40261-015-0328-0 PMID: 26410545
29. Zareba W, McNitt S, Polonsky S, Couderc JP. JT interval: What does this interval mean? Journal of Electrocardiology. 2017; 50:748–751. https://doi.org/10.1016/j.jelectrocard.2017.07.019 PMID: 28942950

30. Darpo B, Couderc JP. Challenges in implementing and obtaining acceptance for J-Tpeak assessment as the clinical component of CiPA. Journal of Pharmacological and Toxicological Methods. 2018 Jun.

31. Vicente J, Zusterzeel R, Johannesen L, Ochoa-Jimenez R, Mason JW, Sanabria C, et al. Assessment of Multi-Ion Channel Block in a Phase I Randomized Study Design: Results of the CiPA Phase I ECG Biomarker Validation Study. Clinical pharmacology and therapeutics. 2019 Apr; 105:943–953. https://doi.org/10.1002/cpt.1303 PMID: 30447156